© 2020. Published by The Company of Biologists Ltd | Journal of Experimental Biology (2020) 223, jeb219980. doi:10.1242/jeb.219980

RESEARCH ARTICLE

Estimation of the force–velocity properties of individual muscles from measurement of the combined plantarflexor properties

Mehrdad Javidi[1], Craig P. McGowan[2,3,4] and David C. Lin[1,4,5,*]

ABSTRACT

The force–velocity (*F–V*) properties of isolated muscles or muscle fibers have been well studied in humans and other animals. However, determining properties of individual muscles *in vivo* remains a challenge because muscles usually function within a synergistic group. Modeling has been used to estimate the properties of an individual muscle from the experimental measurement of the muscle group properties. While this approach can be valuable, the models and the associated predictions are difficult to validate. In this study, we measured the *in situ F–V* properties of the maximally activated kangaroo rat plantarflexor group and used two different assumptions and associated models to estimate the properties of the individual plantarflexors. The first model (Mdl1) assumed that the percent contributions of individual muscles to group force and power were based upon the muscles' cross-sectional area and were constant across the different isotonic loads applied to the muscle group. The second model (Mdl2) assumed that the *F–V* properties of the fibers within each muscle were identical, but because of differences in muscle architecture, the muscles' contributions to the group properties changed with isotonic load. We compared the two model predictions with independent estimates of the muscles' contributions based upon sonomicrometry measurements of muscle length. We found that predictions from Mdl2 were not significantly different from sonomicrometry-based estimates while those from Mdl1 were significantly different. The results of this study show that incorporating appropriate fiber properties and muscle architecture is necessary to parse the individual muscles' contributions to the group *F–V* properties.

KEY WORDS: Muscle architecture, Power–velocity, Muscle modeling, Muscle architecture

INTRODUCTION

The force-generating properties of individual skeletal muscles have been widely studied to understand how muscles enable a variety of motor functions. Furthermore, the properties of the multiple muscles spanning the same joint synergistically combine to determine the moment-generating properties for a particular movement direction. If the individual muscles within a synergistic group have contractile properties that are identical, differ only in size (e.g. physiological cross-sectional area, PCSA) and share a common tendon, the combined properties of the muscle group are a simple weighted sum of the individual muscles. However, in the case of the ankle plantarflexors, substantial differences have been reported among the architectural properties of the individual muscles (i.e. fiber type, pennation angle, optimum length and shortening velocity) (Brown et al., 1996; Close, 1972; Cui et al., 2008) and mechanical properties of their tendons (Cui et al., 2009; Matson et al., 2012). Moreover, rotation of pennation angle as force changes can decrease a muscle's output force but increase output velocity by allowing the muscle to function at a higher gear ratio (Azizi et al., 2008). This implies that the contributions of individual muscles to the total force and power of the group may change with loading conditions. In general, it is not well understood how differences in the properties of individual muscles influence the properties of a group of muscles acting synergistically at a joint (Biewener and Roberts, 2000; Rajagopal et al., 2015).

This gap in knowledge is especially apparent for dynamic conditions, when the force–velocity (*F–V*) properties determine the amount of power that can be delivered over a range of velocities and forces. The relationship between the properties of individual muscles and of the muscle group cannot be calculated unless the properties of individual muscles and the muscle group are measured simultaneously. This is because the alternative of physically separating muscles and measuring their properties is complicated by intermuscular force transmission and/or aponeuroses shared by adjacent muscles (Maas and Sandercock, 2010; Maas et al., 2004; Rijkelijkhuizen et al., 2005; Tijs et al., 2014, 2015, 2016). *In vivo* approaches, such as sonomicrometry or x-ray cinematography, have been used to measure shortening velocity and, in some cases, force in animals but these studies are technically challenging and only provide insight into muscle behavior during specific tasks (Arellano et al., 2016; Biewener and Roberts, 2000; Moo et al., 2017). In human studies, non-invasive *in vivo* experiments have also been used to characterize the moment–velocity relationship at a joint, but often do not break down the contributions of individual muscles (Hill, 1938; Huijing, 1996). Modeling and optimization methods have been used in combination with *in vivo* measurements of the torque–angle and torque–angular velocity of the ankle joint to estimate the properties of individual plantarflexor muscles (Hasson and Caldwell, 2012; Hasson et al., 2011); however, these involve multiple assumptions concerning the model parameters of the muscles and their tendons, many of which cannot be validated experimentally. The limitations of these approaches underscore the need for detailed experimental studies that simultaneously characterize the properties of the group and of the individual muscles to elucidate how individual muscles contribute to the group properties (de Brito Fontana et al., 2018; Epstein and Herzog, 1998; Herzog, 2017).

To demonstrate how the force–length (*F–L*) properties of individual muscles combine to form the group properties, we

[1]Voiland School of Chemical Engineering and Bioengineering, Washington State University, PO Box 646515, Pullman, WA 99164, USA. [2]Department of Biological Sciences, University of Idaho, 875 Perimeter Drive, MS 3051, Moscow, ID 83844, USA. [3]WWAMI Medical Education Program, University of Idaho, 875 Perimeter Drive, MS 4207, Moscow, ID 83844, USA. [4]Washington Center for Muscle Biology, Washington State University, PO Box 646515, Pullman, WA 99164, USA. [5]Department of Integrative Physiology and Neuroscience, Washington State University, PO Box 647620, Pullman, WA 99164, USA.

*Author for correspondence (davidlin@wsu.edu)

M.J., 0000-0002-1209-4812; C.P.M.-G., 0000-0002-5424-2887; D.C.L., 0000-0003-4492-0944

Received 10 December 2019; Accepted 13 July 2020

Journal of Experimental Biology (2020) 223, jeb219980. doi:10.1242/jeb.219980

List of symbols and abbreviations

a_f	curvature of *F–V* curve
F_{GRP}	musculotendon force equal to the muscle group force (N)
$F_{GRP,isot}$	isotonic force of the muscle group (N)
$F_{GRP,max}$	maximum isometric force of the muscle group (N)
F_M	force of muscle M (N)
$F_{M,isot}$	isotonic load of muscle M (N)
$F_{M,max}$	maximum isometric force of the muscle M (N)
$F_{M,n}$	normalized isotonic force of muscle M
GAS	gastrocnemii
k_T	stiffness of individual tendons
l_f	initial fiber length (mm)
$l_{f,M}$	fiber length of muscle M (mm)
L_c	distance between pairs of sonometric crystals inserted into individual muscles (mm)
$L_{c,isot}$	distance between pairs of sonometric crystals at the beginning of isotonic contraction (mm)
$L_{c,o}$	distance between pairs of sonometric crystals during isometric contraction of muscle group (mm)
$L_{c,p}$	distance between pairs of sonometric crystals after passive stretch of muscle group (mm)
$L_{c,s}$	distance between pairs of sonometric crystals at slack length of muscle group (mm)
L_{MT}	musculotendon length equal to distance between origin of muscles and motor arm (mm)
$L_{MT,isot}$	musculotendon length at the beginning of isotonic contraction (mm)
$L_{MT,o}$	actual optimum musculotendon length (mm)
$L_{MT,o}^*$	initial guess of optimal musculotendon length (mm)
$L_{MT,s}$	slack length of the musculotendon unit (mm)
L_{ser}	distance between the servomotor center and the origin of the muscle group (mm)
$L_{T,isot}$	individual tendon length after tendon recoil
$L_{T,o}$	individual tendon length after isometric contraction
$L_{T,s}$	individual tendon length at slack length of the group muscle
LG	lateral gastrocnemius
MG	medial gastrocnemius
MT	musculotendon unit
$PCSA_{GRP}$	physiological cross-sectional area of the muscle group (mm^2)
$PCSA_M$	physiological cross-sectional area of muscle M (mm^2)
P_{GRP}	power of the muscle group (W)
$P_{GRP,max}$	maximum power of the muscle group (W)
$P_{M,max}$	maximum power of muscle M (W kg^{-1})
PL	plantaris
SOL	soleus
V_f	shortening velocity of an individual muscle's fibers (m s^{-1})
$V_{f,n}$	normalized fiber shortening velocity (s^{-1})
$V_{f,n\text{-}max}$	maximum normalized fiber shortening velocity (s^{-1})
V_{max}	maximum velocity
V_M	shortening velocity of muscle M (m s^{-1})
V_{MT}	shortening velocity of the musculotendon unit (mm s^{-1})
$V_{MT,max}$	shortening velocity of the musculotendon unit associated with zero force (mm s^{-1})
$V_{MT,n}$	normalized shortening velocities of the muscle group
$V_{MT,o}$	optimum shortening velocity of the musculotendon unit
ΔL_c	change in distance between pairs of sonometric crystals
$\Delta L_{c,o\text{-}isot}$	change in distance between the pair of sonometric crystals of an individual muscle from isometric to start of isotonic contractions (mm)
$\Delta L_{c,p\text{-}o}$	change in distance between pairs of sonometric crystals of individual muscles during isometric contractions (mm)
$\Delta L_{c,s\text{-}p}$	change in distance between pairs of sonometric crystals of individual muscles from slack length to passive stretch (mm)
ΔL_{MT}	change in musculotendon length (mm)
$\Delta L_{MT,o\text{-}isot}$	change in musculotendon length from the optimum length to the isotonic contraction (mm)
$\Delta L_{MT,s\text{-}o}$	change in musculotendon length from the slack length to the optimum length of the group (mm)
ΔL_T	change in tendon length (mm)
θ_M	pennation angle of muscle M (deg)
$\sigma_{GRP,max}$	muscle group maximum stress (kPa)

previously studied the plantarflexors of kangaroo rats under static conditions (Javidi et al., 2019a). Briefly, the kangaroo rat plantarflexors are an excellent model for addressing how muscles work together at a single joint for two reasons. First, they deliver the greatest contribution to the power of a vertical jump (Schwaner et al., 2018), and thus they all are likely synergistically maximally activated during jumping. Second, the soleus (SOL) is the only uniarticular plantarflexor and is very small in kangaroo rats (about 2% of total plantarflexor mass; Biewener and Blickhan, 1988; Biewener et al., 1988; Rankin et al., 2018), so it can be removed without greatly affecting plantarflexor capacity. The remaining plantarflexors, the lateral and medial gastrocnemii and plantaris (LG, MG and PL, respectively), have origins almost at the same place on the femur and are likely to have predominantly fast-type muscle fibers typical of small rodents (Schiaffino and Reggiani, 2011), and their distal tendons attach to approximately the same point on the calcaneus (Rankin et al., 2018). It is also very important to note that in kangaroo rats, the tendons of the LG and MG (i.e. the gastrocnemii, GAS) merge together but the tendon of the PL can be easily separated from the other two; thus, the PL tendon is mechanically independent of the LG and MG tendons (Javidi et al., 2019b).

In this study, our objective was to estimate the *F–V* relationships of the individual muscles of the plantarflexors of kangaroo rats from the measured *F–V* relationship of plantarflexors as a group, which was characterized by the standard *in situ* technique of applying isotonic loads. To perform this estimation, two different models based on two different assumptions about the contributions of individual muscles to group output were used. In the first model, we assumed that each muscle's percent contribution (based upon cross-sectional area) to the group *F–V* relationship would be constant across all group forces. The second model assumed that the *F–V* relationships for the fibers of each individual muscle were identical, which would change each muscle's percent contribution according to the group force (due to differences in architectural parameters amongst muscles). In addition, comparisons of the two model predictions were made to independently derived estimates of force levels of individual muscles based upon the length changes in tendons, which were calculated from sonomicrometry data during the isotonic experiments. By comparing the model predictions with an independent estimate, we could test the hypothesis that inclusion of appropriate fiber properties and muscle architecture is necessary to separate the individual muscle contributions across different force levels.

MATERIALS AND METHODS

Animals

All procedures completed were approved by the Institutional Animal Care and Use Committee (IACUC) at Washington State University. Experiments were performed with seven wild-caught adult kangaroo rats, *Dipodomys deserti* Stephens 1887 (4 males, 3 females, mean±s.d. mass 102.9±22.58 g, age unknown).

Surgical procedure and experimental setup

The surgical procedure and experimental setup were similar to our previous study on the *F–L* properties of kangaroo rat plantarflexors (Javidi et al., 2019a); thus, they will be briefly described here. Animals were anesthetized with inhalant isoflurane (1%) and an intraperitoneal injection of 50 mg kg^{-1} ketamine and 0.15 mg kg^{-1} dexmedetomidine. The plantarflexor muscles of the right leg with their tendons were dissected from surrounding muscles and tissues, leaving the proximal end attached to the femur, major blood vessels intact, and the distal tendons attached to the calcaneus, which was

later cut to create a bone chip attached to the tendon. The SOL muscle was removed from the rest of the plantarflexors because it was very small relative to the other plantarflexors (see Introduction). The sciatic nerve was cut proximally (near the hip joint) and distally, the tibial branch was left intact and the other branches (i.e. sural and common peroneal) were cut. To sonometrically measure the muscle belly length changes of the LG, MG and PL, a pair of piezoelectric crystals (1.0 mm diameter; Sonometrics) were implanted near the proximal and distal aponeurosis of each muscle of 5 animals (see Fig. 1A, white circles on LG as an example). The servomotor (309C; Aurora Scientific, Aurora, ON, Canada) measured both force and position at 1000 Hz (Real-Time Muscle Data Acquisition, Aurora Scientific, Aurora, ON, Canada) and was connected to the Achilles tendon via a hook clipped onto the bone chip.

To mechanically ground the origin of the muscle group, a stainless steel intramedullary pin (0.7 mm o.d.) was inserted through the femur and its ends were then secured to a custom-fabricated support arm attached to the animal platform. A wire loop (0.5 mm o.d.) was wrapped around the middle of the femur and support arm to prevent any horizontal displacement of the femur. The muscle group was immersed in a custom-made temperature-controlled (37°C) trough of mineral oil for the duration of testing to prevent muscle dehydration and maintain temperature. The calcaneal bone chip was then attached to the lever-arm of the servomotor and the sciatic nerve was placed onto custom-made bipolar hook electrodes (0.3 mm silver wire). A rectal temperature probe and pulse oximeter (PhysioSuite; Kent Scientific, Torrington, CT, USA) placed on the paw allowed for continuous monitoring of core body temperature, oxygenation level and heart rate.

Experimental protocols

Servomotor force [equivalent to musculotendon (MT) force, F_{GRP}], servomotor arm position relative to its initial position (equivalent to the change in musculotendon length, ΔL_{MT}) and distance between the pairs of sonometric crystals inserted into individual muscles (L_c) (Fig. 1) were recorded at 1000 Hz.

Before the active muscle measurements, the motor arm was fixed vertically (ΔL_{MT}=0), and the motor was moved until the passive force of the muscle group was equal to a very small positive value. The distance between the servomotor center and the origin of the muscle group (L_{ser} in Fig. 1A) was then measured by calipers and defined to be the slack length of the muscle–tendon unit ($L_{MT,s}$). Distances between the sonometric crystal pairs of individual muscles also were collected at this time. We used the slack length as the initial guess of optimal MT length ($L_{MT,o}$*).

We determined the actual optimum MT length of the group ($L_{MT,o}$) so that the isotonic measurement could be made near optimal length to minimize any F–L effects. To do so, the isometric force of the muscle group was measured at a minimum of seven different random MT lengths within a range of L_{MT}=$L_{MT,o}$*+ΔL_{MT}, where $-4 \leq \Delta L_{MT} \leq +3$ mm, using supramaximal isometric tetanic contractions generated by 300 ms trains of 0.2 ms biphasic pulses at 150 Hz. We fitted a polynomial curve to the active force and length data, and the optimum MT length ($L_{MT,o}$) and the maximum isometric force of the group ($F_{GRP,max}$) were estimated from the values associated with the peak of the fitted curve (more detailed methods are found in Javidi et al., 2019a; Rehwaldt et al., 2017). Subsequently, all isotonic trials were started at $L_{MT,o}$ (Fig. 1).

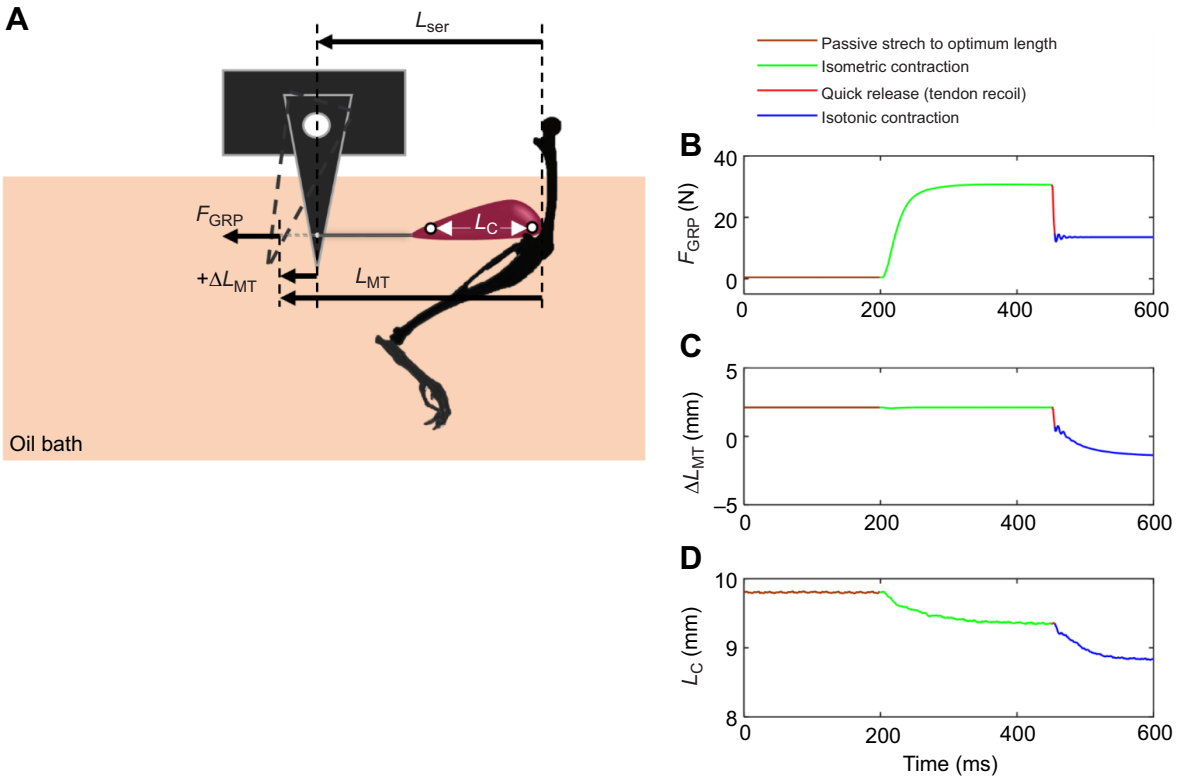

Fig. 1. Schematic diagram of the experimental setup and a sample of raw data. (A) F_{GRP}, force measured by the servomotor; L_{ser}, position of the servomotor with respect to the origin of muscle group; ΔL_{MT}, change in the vertical position of motor arm with respect to its vertical position, which is equal to the change in the group muscle–tendon (MT) length; and L_c, distance between crystal pair inserted into the muscle. L_{MT}, the group MT length, was calculated by the following equation: L_{MT}=L_{ser}±ΔL_{MT}. (B–D) Samples of collected data for (B) measured force, (C) change in MT length and (D) distance between the pair of sonometric crystals inserted into the plantaris (PL).

Isotonic quick-releases were performed with a minimum of 6 isotonic levels, with 9 levels being typical and not exceeded. These levels were relative to maximal tetanic force ($F_{GRP,max}$) and within a range of 0.1–1.0 $F_{GRP,max}$. We could not use a level of zero force because overshoot in the servomotor caused an artifact as the MT went slack. For each level, the MT was stretched to $L_{MT,o}$ and we elicited an isometric supramaximal tetanic contraction with a 250 ms train of 0.2 ms biphasic pulses at 150 Hz (Fig. 1). The servomotor then switched from length control to force control and isotonic tetanic shortening occurred for a 150 ms interval. Isotonic levels were randomized and muscles were rested for 3 min between each level. At the end of the experiment, animals were terminally anesthetized, muscles were dissected from their tendon and each muscle mass was measured.

Calculation of muscle group properties

Data analysis

The objective of the data analysis was to estimate the *F–V* curve by calculating the velocity and force following the application of the isotonic load, when it is assumed that velocity and force have reached a steady state. For each isotonic level, ΔL_{MT} was fitted with a line from 10 to 25 ms following the force drop (Fig. 1C) to estimate shortening velocity of the musculotendon (V_{MT}). The isotonic force of the muscle group ($F_{GRP,isot}$) was also calculated for the same time interval (Fig. 1B).

Calculation of *F–V* and power–velocity properties

For each animal, isotonic forces of the muscle group and shortening velocities were fitted to a rectangular hyperbolic curve using Hill's equation (Hill, 1938):

$$F_{GRP} = b((F_{GRP,max} + a)/(V_{MT} + b)) - a, \quad (1)$$

where F_{GRP} and V_{MT} are the isotonic force and shortening velocity of the muscle group, respectively; a and b are constants with units of force and velocity, respectively. Using the fitted curve, $V_{MT,max}$ was estimated as the velocity associated with zero force. Power of the muscle group (P_{GRP}) was calculated as:

$$P_{GRP} = F_{GRP} \times V_{MT}, \quad (2)$$

where F_{GRP} was calculated from Eqn 1 and V_{MT} was shortening velocity of the muscle group. P_{GRP} and V_{MT} were then used to generate the P_{GRP}–V_{MT} curve.

To pool the muscle group *F–V* and power–velocity (*P–V*) relationships across animals, V_{MT} was normalized by $V_{MT,max}$ and $F_{GRP,isot}$ was normalized by $F_{GRP,max}$ for each animal's data. The pooled normalized *F–V* data were fitted to the rectangular hyperbolic curve (Eqn 1). Note that in Eqn 1, $F_{GRP,max}$ and V_{MT} were replaced by 1 and normalized velocities, respectively. The normalized *P–V* relationship was calculated as the product of the normalized forces and velocities.

Estimates of individual muscle properties based on muscle group properties

The normalized F_{GRP}–V_{MT} relationship for the data pooled across animals was then used to estimate the *F–V* curves of the LG, MG and PL. Briefly, we used two sets of assumptions that resulted in two different models, which we called Mdl1 and Mdl2. An overview of how we used the two models is shown in Fig. 2 and described in detail below.

Calculation of muscle velocity

In both models, it was assumed that the isotonic shortening velocities of individual muscles were equal to the shortening velocity of the muscle group [i.e. V_{MT}=V_M=V_{PL}=V_{MG}=V_{LG}, where the subscript indicates the velocity of the MT, an individual muscle within the group (M), or a specific muscle (PL, LG or MG)] as there should be no length changes in the individual tendons because of the constant force conditions. To estimate the shortening velocity of an individual muscle's fibers from the muscle velocity, we assumed that:

$$V_f = V_M/\cos(\theta_M), \quad (3)$$

where V_M and θ_M are the shortening velocity and pennation angle of the individual muscles.

Calculation of individual muscle force and power

Because of the parallel arrangement of the individual muscle–tendon units of kangaroo rat plantarflexors (see Introduction), the sum of the force and of the power generated by individual muscles are assumed to be equal to the force and power of the group, which

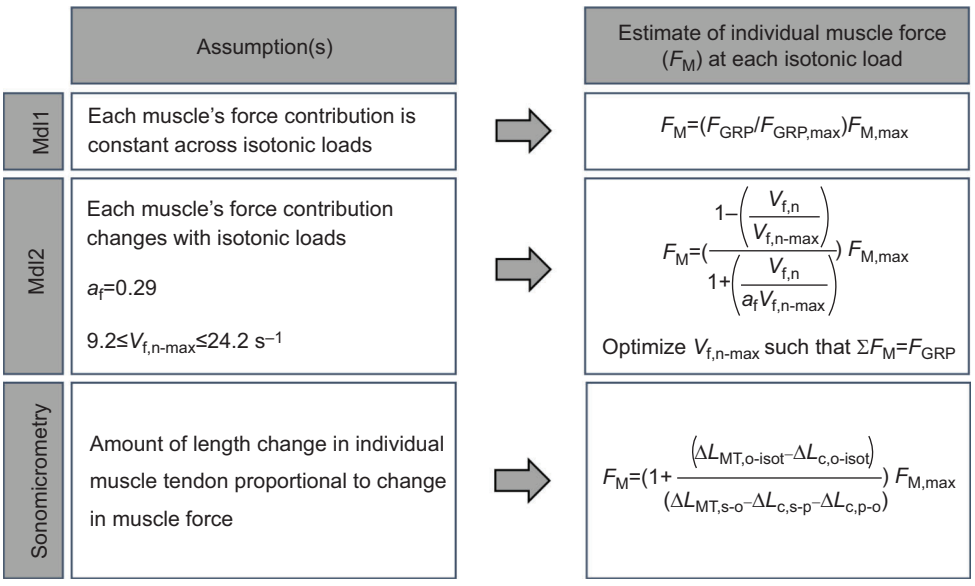

Fig. 2. Overview of the two models (Mdl1 and Mdl2) and sonomicrometry-based measurements used to estimate forces in individual muscles. See 'List of symbols and abbreviations' for definitions. In Mdl1, the force contribution of each muscle at each isotonic load was a proportion of the total group force, with a proportionality constant based on its physiological cross-sectional area (PCSA). In Mdl2, the individual muscle contributions to the group force were estimated based on the forces calculated from the assumption that all the muscles had identical fiber properties but different architectural parameters. In the sonomicrometry-based calculations, the length changes in tendons were used to calculate the forces generated by individual muscles.

were calculated by Eqns 1 and 2, respectively:

$$F_{GRP} = \sum F_M, \quad (4)$$

$$P_{GRP} = \sum (F_M \times V_M), \quad (5)$$

where F_M and V_M are the isotonic load and shortening velocity of the individual muscles (i.e. PL, MG or LG).

In Mdl1, we assumed that each muscle's percent contribution (based on PCSA; see below) to the group F–V relationship would be constant across all group forces (Fig. 2). In other words, the normalized F–V relationships of individual muscles were assumed to be the same as the normalized F–V relationship of the muscle group. In Mdl2, we assumed that the normalized F–V relationships of the fibers within each individual muscle were identical, and this would result in a change in each muscle's percent contribution according to the group force (as a result of differences in architectural parameters among muscles). For example, fiber length scaled the normalized F–V relationship, so that differences in fiber length between muscles resulted in differences in predicted force for a given absolute velocity. Because the kangaroo rat plantarflexors are likely all fast fibers (Graffe et al., 2017), we used a value of 0.29 for the curvature of the F–V curve (a_f), which is appropriate for fast fibers based upon a literature survey of 59 species (Dick et al., 2017). To find the normalized (by initial fiber length, l_f) maximum fiber shortening velocity ($V_{f,n\text{-}max}$), we optimized $V_{f,n\text{-}max}$, such that the summation of forces of the individual muscles, which were calculated by using the F–V equation (Eqn 1) scaled by fiber length and maximum isometric force (see below), were equal to the group force for all velocities (Fig. 2). The guess of $V_{f,n\text{-}max}$ was then optimized until model calculation of the group force matched the experimental measurement of group force.

Maximum isometric force of individual muscles

In both models, the contribution of individual muscles to the maximum isometric group force was estimated from the cross-sectional area of each muscle and the assumption that all three muscles have the same specific tension. Therefore, the contribution of an individual muscle to the maximum isometric force of the group was calculated by:

$$F_{M,max} = (PCSA_M/PCSA_{GRP}) \times F_{GRP,max}, \quad (6)$$

where $PCSA_{GRP}$ is the PCSA of the muscle group and was assumed to be equal to the summation of $PCSA_M$ of the individual muscles. PCSA was calculated by:

$$PCSA_M = (m \times \cos(\theta_M))/(l_{f,M} \times \rho), \quad (7)$$

where ρ is the density of mammalian muscle of 1.06 mg mm^{-3} (Mendez and Keys, 1960), $l_{f,M}$ is the fiber length and θ_M is the pennation angle of the muscle. In our study, we used the fiber lengths $l_{f,PL}$=8.8 mm, $l_{f,LG}$=16 mm and $l_{f,MG}$=13.7 mm and pennation angles θ_{PL}=22.8 deg, θ_{LG}=18.8 deg and θ_{MG}=22.6 deg, measured from a large sample of kangaroo rats with the same mass range as those used in this study (Rankin et al., 2018).

Contribution of individual muscles to muscle group properties

In both models, the velocity of individual muscles was assumed to be equal to that of the muscle group. The force of individual muscles at each level of isotonic load or constant shortening velocity of the muscle group also was estimated by models. These estimations of the force with the velocity can simply be used to calculate percent contributions of individual muscles to the muscle group force and power.

Estimates of individual muscle properties based on sonomicrometry data

The general basis for the calculation of F–V properties based on sonomicrometry data was using the amount of tendon stretch and recoil during the isotonic protocol to estimate force in each muscle. Specifically, similar to the models explained above, we assumed that the shortening velocities of individual muscles were equal to the shortening velocity of the muscle group. Then, for each isotonic trial, the length of MT and distances between crystal pairs inside individual muscles were calculated in three conditions (see Fig. 1). The initial condition was when the muscle group was at its slack length, and the distances between the pairs of sonometric crystals inserted into the individual muscles were calculated as $L_{c,s}$. The maximum isometric contraction condition included two different parts: the passive stretch of the muscle group to its optimum length (Fig. 1, brown solid lines) and then the isometric contraction (Fig. 1, green solid lines). The optimum musculotendon length ($L_{MT,o}$), and the individual crystal distances after passive stretch ($L_{c,p}$) and after isometric contraction ($L_{c,o}$) were measured in the isometric condition. The last condition was immediately after the tendon recoil phase (Fig. 1C,D, red solid lines), when the MT length ($L_{MT,isot}$) and crystal distance of individual pairs ($L_{c,isot}$) were measured.

The estimates of force in the individual muscles for each isotonic trial was made by assuming that the tendon attached to each muscle acted as a linear spring, and therefore force was proportional to tendon length change. In other words, the muscle force could be calculated from the amount of tendon recoil immediately following the imposition of the isotonic load (Fig. 1C,D, red solid lines). More specifically, we estimated the normalized isotonic force ($F_{M,n}$) of individual muscles, i.e. the force of a muscle ($F_{M,isot}$) divided by its maximum isometric force ($F_{M,max}$). Using the assumption stated above, $F_{M,n}$ would then be equal to the amount of stretch in the individual tendons at isometric contraction over the amount of tendon recoil (see Appendix):

$$F_{M,n} = 1 + \frac{(\Delta L_{MT,o\text{-}isot} - \Delta L_{c,o\text{-}isot})}{(\Delta L_{MT,s\text{-}o} - \Delta L_{c,s\text{-}p} - \Delta L_{c,p\text{-}o})}, \quad (8)$$

where $\Delta L_{MT,s\text{-}o}$ and $\Delta L_{MT,o\text{-}isot}$ are the changes in MT length from the slack length to the optimum length of the group (Fig. 1C, green solid line) and from the optimum length to the isotonic contraction ($\Delta L_{MT,o\text{-}isot}$ was equal to the amount of change in the red solid line, Fig. 1C), respectively. $\Delta L_{c,s\text{-}p}$, $\Delta L_{c,p\text{-}o}$ and $\Delta L_{c,o\text{-}isot}$ are the changes in distance between the pair of sonometric crystals of individual muscles from slack length to passive stretch, shortening during isometric contraction and from isometric to the start of isotonic contractions, respectively. Note that because this method calculates the isotonic force as force normalized by the isometric force, it does not require knowledge of the specific value of tendon stiffness (i.e. tendon stiffness cancels in the numerator and denominator of the formulation of Eqn 8). To separate the contributions of the LG and the MG, we also had to assume that their tendons were effectively independent, and as a consequence, the muscle length changes (as measured by sonomicrometry) were influenced by the apparent stiffness of the tendon attached to each muscle.

Sonomicrometry was performed on 5 animals. The normalized forces of individual muscles ($F_{M,n}$) and the normalized shortening

velocities of the muscle group ($V_{MT,n}$) for 5 animals were pooled and fitted to a rectangular hyperbolic curve (Eqn 1).

Statistics

The error metrics were calculated as the absolute values of the difference between each point from sonomicrometry data, as well as between each point from sonomicrometry data and the *F–V* relationships predicted by Mdl1 and Mdl2. Then, the mean errors were used in an ANOVA table to test whether the method to estimate muscle force (Mdl1, Mdl2 or sonomicrometry) had a significant effect on the predictions of individual muscle properties. If the effect was significant ($P<0.05$), the methods were compared with the Tukey–Kramer test using the multicompare function of MATLAB to find which paired comparison had a significant difference at a level of 0.05.

RESULTS

Results (presented as means±s.d.) are the data from 7 animals. The mass of the PL, MG and LG muscles was 0.35±0.09, 0.48±0.12 and 0.48±0.10 g, respectively. The calculated PCSA of the PL, MG and LG muscles was 34.30±9.90, 30.54±8.01 and 27.14±5.88 mm^2, respectively.

Muscle group properties

The muscle group *F–V* and the *P–V* curves of each animal were fitted to Hill's equation to visualize the variability across all animals (Fig. 3A,B). The means of $F_{GRP,max}$ and $V_{MT,max}$ were 25.63±5.83 N and 146.54±41.97 mm s^{-1}, respectively. By using the maximum isometric force of the group and its PCSA, the maximum stress of the kangaroo rat plantarflexors combined was 283±37.8 kPa. The mean maximum power ($P_{GRP,max}$) and optimum shortening velocity of the MT ($V_{MT,o}$) were 335.02±89.49 mW and 43.54±8.95 mm s^{-1}, respectively. Normalized *F–V* and *P–V* data from all animals were pooled and fitted to Hill's equation (Fig. 3C,D). The maximum power of the muscle group normalized to the weight of plantarflexors was 255±24.86 W kg^{-1}. The curvature ($a/F_{GRP,max}$) of the fitted normalized *F–V* curve was 0.24.

Estimates of individual muscle properties based on muscle group properties

The normalized force and fiber *F–V* relationships and the normalized *P–V* relationships of individual muscles were estimated by the two models (Fig. 4). The differences between the estimates of the individual muscle properties by the different models, specifically for PL and LG are clear (Fig. 4A,C). The properties of individual muscles estimated by the two different models are given in Table 1. By using the calculated PCSAs and Eqn 6, the maximum isometric force of PL, MG and LG was estimated as 37.3%, 33.2% and 29.5% of $F_{GRP,max}$.

Contribution of individual muscles to muscle group properties

Noticeable differences were observed between the contributions of individual muscles to the group force and power at different isotonic levels predicted by the two models (Fig. 5). Specifically, at lower isotonic levels (or higher MT velocities), Mdl2 predicted a decrease in the contribution of PL to the muscle group force (or power), while for Mdl1, the contribution remained constant (Fig. 5E,F). Similarly, there was an increase in contributions by the MG and LG as isotonic level decreased for Mdl2, while they remained constant for Mdl1.

Comparisons between the predictions from the models and sonomicrometry data

The forces of individual muscles normalized by their maximum isometric forces at different isotonic levels of the muscle group were estimated from the sonomicrometry data and fitted to Hill's equation (Fig. 6). The statistical analysis indicated that the models have significant effects on the predictions of the isotonic load of individual muscles ($P=0.001$). The individual group comparison (Table 2) indicated that the prediction of Mdl1 was significantly different from

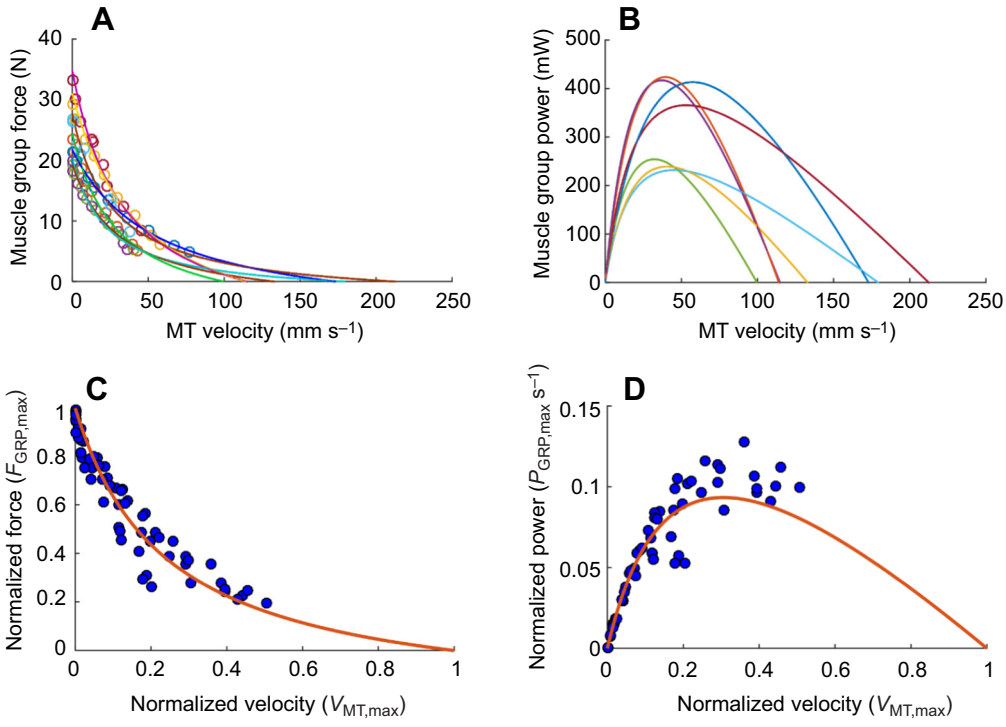

Fig. 3. The force–velocity (*F–V*) and power–velocity (*P–V*) curves of the muscle group. (A) *F–V* relationships of the group muscle properties for all individual animals ($n=7$). (B) *P–V* relationships of the group muscle properties for all individual animals. (C) Normalized force and velocity of group muscle (blue circles) and fitted curve (red solid line) for all animals pooled. (D) Normalized power and velocity of group muscle (blue circles) and fitted curve (red solid line).

Journal of Experimental Biology (2020) 223, jeb219980. doi:10.1242/jeb.219980

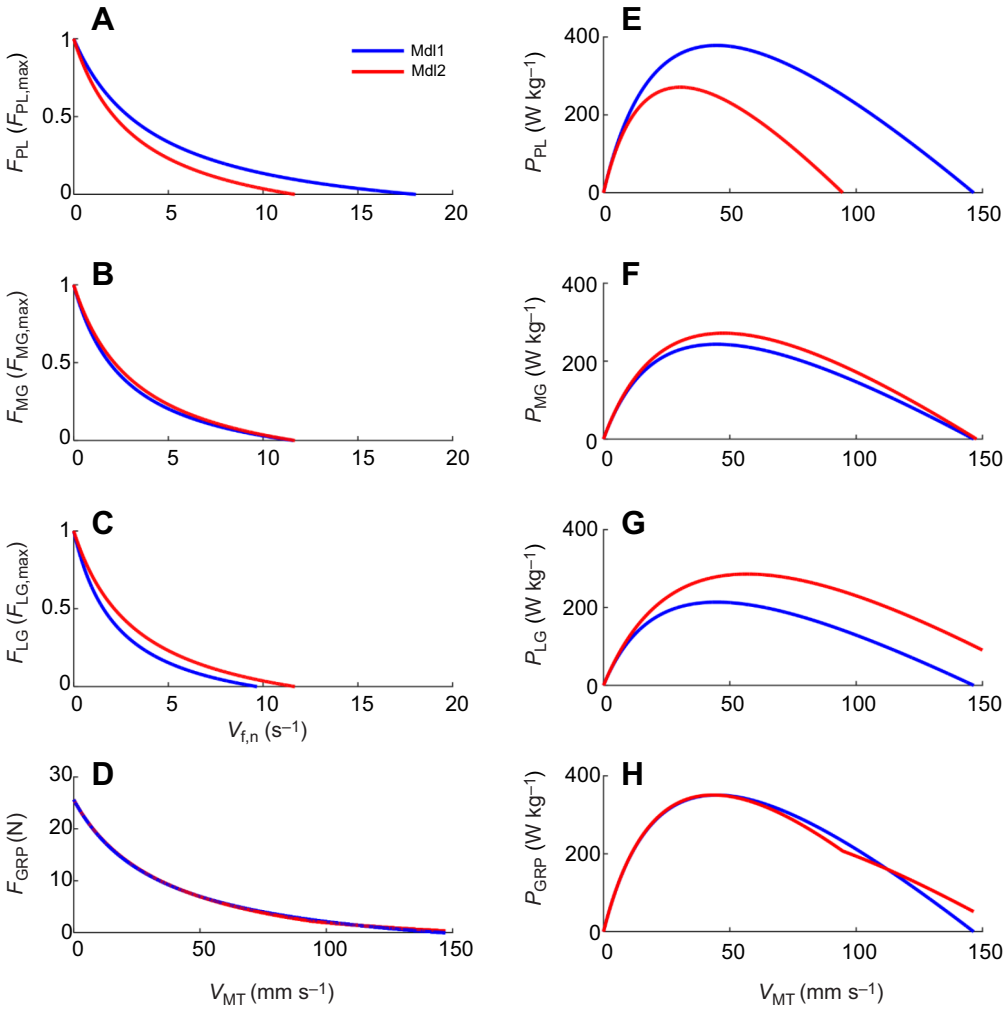

Fig. 4. Properties of individual muscles and the muscle group predicted by the two models. (A–D) Normalized force and normalized velocity relationships of the fibers of individual muscles (PL, plantaris; MG, medial gastrocnemius; LG, lateral gastrocnemius) and the *F–V* relationship of the muscle group predicted by two different models. (E–H) Normalized power and velocity relationships of the individual muscles and the *P–V* relationship of the muscle group predicted by two different models. See 'List of symbols and abbreviations' for definitions.

the fitted curve to sonomicrometry-based data (P=0.0007) while there was no significant difference between the Mdl2 prediction and sonomicrometry-based calculation (P=0.4690).

DISCUSSION

The motivation of this study was to address the challenges involved with estimating the contributions of individual muscles within a synergistic group, especially under *in vivo* conditions when it is only possible to measure the mechanical output from the group. By comparing model predictions with independent estimates of the *F–V* curves, we tested the hypothesis that the measured properties of the kangaroo rat plantarflexor muscle group could be used to estimate the *F–V* and *P–V* relationships of individual muscles, if muscle-specific architecture is incorporated into a model.

Contractile properties of the plantarflexors

There was variation in the absolute maximum shortening velocity and maximum power of the plantarflexor muscles as a group for 7 animals (Fig. 3A,B). The animals used in this study were different in sex, size and likely age, which was unknown because they were wild caught. Any of these factors could have effects on the performance of the muscles and the absolute values of the maximum isometric force, maximum shortening velocity and maximum power. However, the variation decreased by normalizing the values (Fig. 3C,D).

Moreover, variation in the *F–V* curves likely arose from the difficulty in collecting data at low isotonic levels without artefacts due to oscillations from the servomotor (see Materials and Methods). By not including data from the lowest isotonic forces, we could have underestimated the maximum shortening velocities obtained from curve fitting (Marsh and Bennett, 1986). Practically speaking, we preferred to estimate the curve shape and its maximum based on the more reliable forces that were collected at a higher level of the forces. Furthermore, to minimize the effects of the transition from isometric to isotonic load and to maintain consistency in our analysis, we measured the velocity within the period of 10–25 ms

Table 1. Estimation of individual muscle properties by the two different models

	$V_{f,n\text{-}max}$ (s^{-1})			$V_{MT,o}$ (mm s^{-1})			$P_{M,max}$ (W kg^{-1})		
Model	PL	MG	LG	PL	MG	LG	PL	MG	LG
Mdl1	18.06	11.59	9.68	45.57	45.13	43.52	378	243	213
Mdl2	11.68	11.68	11.68	30.65	47.09	56.57	271	271	286

PL, plantaris; MG, medial gastrocnemius; LG, lateral gastrocnemius. For other definitions, see 'List of symbols and abbreviations'.

Journal of Experimental Biology (2020) 223, jeb219980. doi:10.1242/jeb.219980

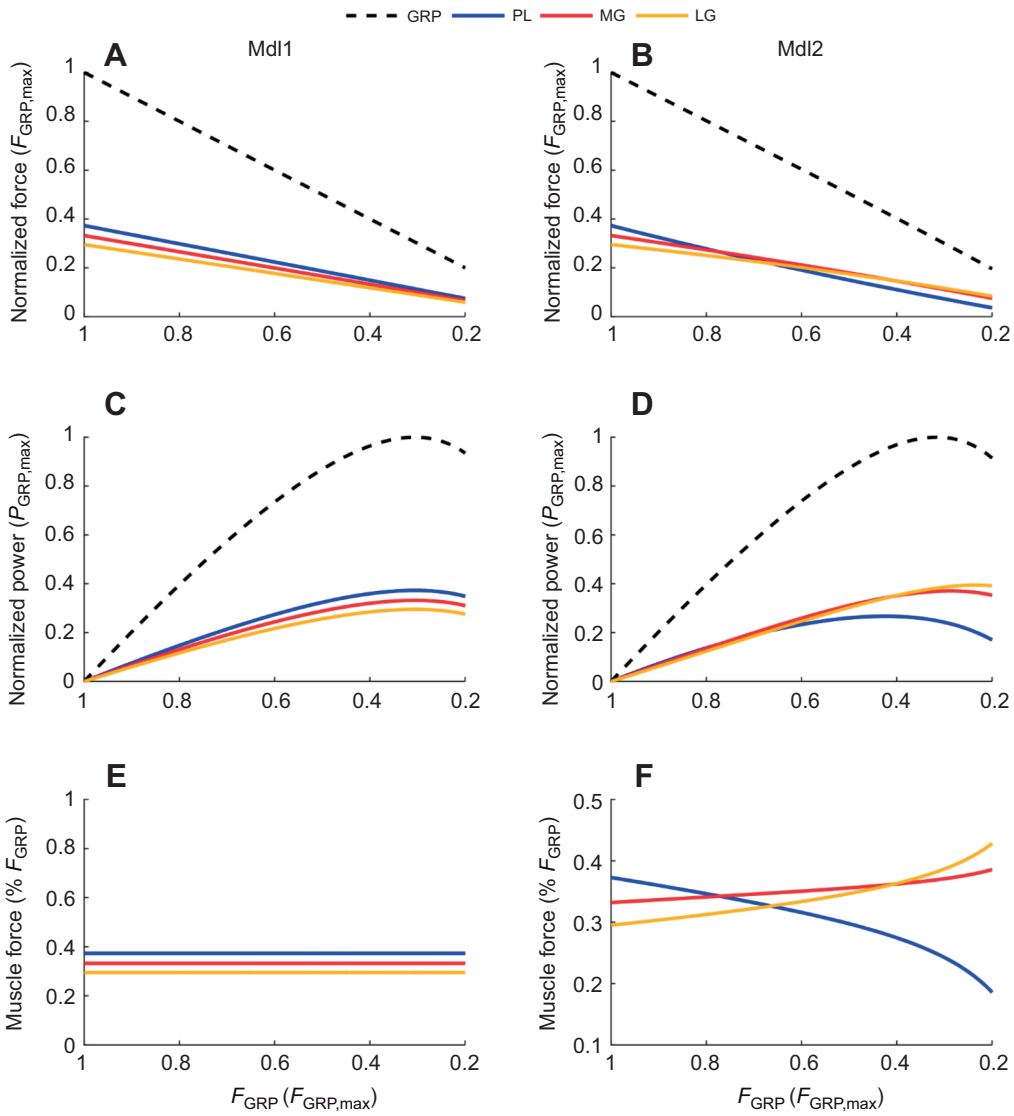

Fig. 5. Contribution of individual muscles to the group muscle force and power predicted by Mdl1 (left) and Mdl2 (right). (A,B) Contribution of individual muscles to the group muscle force. (C,D) Contribution of individual muscles to the power of the muscle group. (E,F) Contribution of individual muscles to the group muscle force (power will be the same with these curves) at different isotonic levels of the group muscle load.

for all trials, which may have led to an underestimation of the isotonic velocity.

Our estimate of muscle group maximum stress $\sigma_{GRP,max}$=283±37.8 kPa is very similar to the value we measured in the study of the *F–L* properties of kangaroo rat plantarflexor (Javidi et al., 2019a). This value was slightly larger than specific tensions from *in situ* experiments on the SOL, PL and GAS of several species, such as mouse, rat, rabbit, cat and hopping mouse, which were measured in the range from 150 to 250 kPa (with a few exceptions) (Rospars and Meyer-Vernet, 2016). This discrepancy may be due to the calculation of specific tension by muscle cross-sectional area (without the correction for pennation angle, Eqn 7). The specific tension values without accounting for pennation angle were $\sigma_{GRP,max}$=263±35.1 kPa.

The values reported for maximum intrinsic speed ($V_{f,n\text{-}max}$) of mouse, cat and rat muscle measured at physiological temperatures have a large amount of variability in that they range from 4.8 to 7.3 s^{-1} for slow fibers and from 9.2 to 24.2 s^{-1} for fast fibers (Dick et al., 2017; Medler, 2002). The values of the maximum shortening velocity of the individual muscles, estimated by either Mdl1 or Mdl2 (Table 1), were consistent with the fast fiber type data of similarly sized species. This conclusion is also supported by a preliminary electrophoresis study which showed the LG was composed entirely of fast myosin heavy chain isoforms (Graffe et al., 2017).

Pennation angle has been shown to change with length and load (Azizi et al., 2008), and this affects the calculation of fiber velocity, specifically when converting muscle velocity to fiber velocity. We did not factor in this effect in the current study, and we used a constant pennation angle at all levels of force. An increasing pennation angle at smaller isotonic loads would have increased the estimation of fiber velocity (for a given muscle velocity; see Eqn 3) and produced a larger estimate of maximum velocity, V_{max}.

The maximum power output of vertebrate skeletal muscles has been reported to be in the range from 150 to 480 W kg^{-1} (Askew and Marsh, 1998; Nelson et al., 2004; Rehwaldt et al., 2017; Sawicki et al., 2015; Swoap et al., 1997; Weis-Fogh and Alexander, 1977). Previous studies of the jumping performance by kangaroo rats (Biewener and Blickhan, 1988; Schwaner et al., 2018) estimated maximum power in individual muscles to be within this range of reported values and concluded that kangaroo rat muscles are not comparatively more powerful. The maximum power that was calculated here by the two different models either for the muscle group or for the PL, LG and MG individually (Table 1) also did not exceed this range.

Journal of Experimental Biology (2020) 223, jeb219980. doi:10.1242/jeb.219980

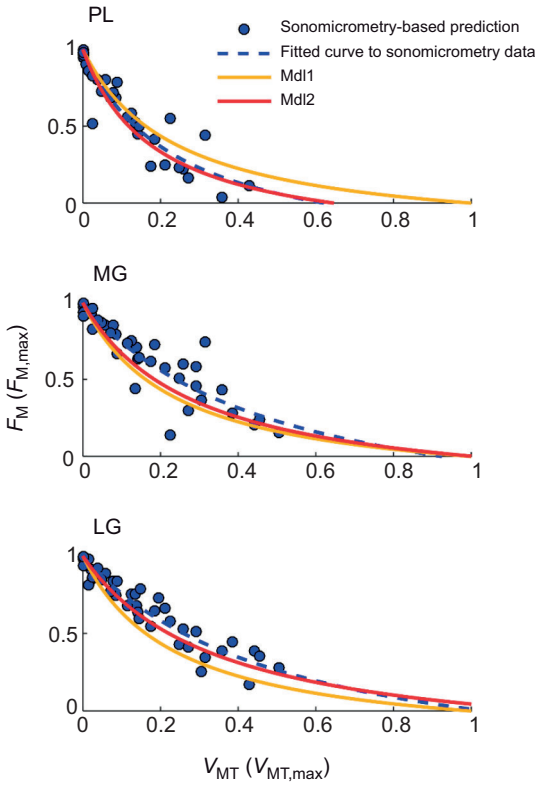

Fig. 6. Comparison between model predictions and sonomicrometry-based estimation. Amount of isotonic load at different shortening velocities of the MT estimated by sonomicrometry data (blue circles, *n*=5) and a curve fitted to these data (blue dashed line). The same relationships predicted by the two different models are also shown for comparison.

Accuracy of the estimated muscle *F–V* properties

We estimated the *F–V* properties of each muscle from a measurement of the group *F–V* properties using two models, with each model having a different set of assumptions. Mdl1 assumed that the percent contribution of each muscle to the group *F–V* does not change with isotonic level. For example, this assumption has been used to measure the contribution of vastus lateralis muscle to moments generated by isokinetic contraction of knee extensors (Ichinose et al., 2000). Although this approach is not theoretically correct (de Brito Fontana et al., 2018; Herzog, 2017), we wanted to see how much the predication would be different from Mdl2 and the estimation based on sonomicrometry measurements. Mdl2 assumed that the fiber *F–V* properties were identical, but because of muscle architectural differences, the muscles would operate on different portions of the fiber *F–V* curves for different isotonic levels. As a result, the percent contribution of each muscle to the group force would change as the isotonic level (and shortening velocity) changed. In fact, the PL does not contribute any force at the lowest isotonic levels because the high group muscle velocity results in a fiber velocity greater than the PL's V_{max}. The assumptions of Mdl2 are commonly used in musculoskeletal models to estimate *F–V* relationships of individual muscles from the torque angular velocity relationship at the joint (Anderson et al., 2007; Caldwell and Chapman, 1991; Garner and Pandy, 2003). Although these methods also can be combined with imaging techniques to estimate more realistic model parameters (Fukashiro et al., 1995; Hasson and Caldwell, 2012; Rugg et al., 1990), it is not possible to measure all musculoskeletal parameters experimentally. Like these other studies, we could not measure all the muscle parameters directly in that we needed to optimize the parameter of fiber maximal shortening velocity, and this produced uncertainty in the model predictions.

Table 2. Statistical comparison between the sonomicrometry-based estimation and predictions by the two models

	Average of absolute error±s.e.m.		
	PL	MG	LG
Mdl1	0.083±0.013[a,b]	0.107±0.014[c,d]	0.106±0.012[e,f]
Mdl2	0.074±0.013[a]	0.092±0.013[c]	0.063±0.008[e]
Sonomicrometry	0.069±0.013[b]	0.069±0.013[d]	0.057±0.006[f]

For each muscle (columns), predictions of Mdl1 were significantly different from either the predictions of Mdl2 or the sonomicrometry estimates. The predictions of Mdl2 and sonomicrometry estimates were not significantly different. (Significant differences at the confidence level of 0.05 are shown by different superscripts.)

We made the assumption that in both Mdl1 and Mdl2, GAS and PL muscle–tendon units are two independent actuators with the same mechanical actions in the sagittal plane, thus the total force of the group is equal to the sum of the force generated by individual muscles and transferred through their tendons (see Eqn 4). However, force transmission between muscle–tendon units through the connective tissue due to the relative displacement of the muscles (Maas and Sandercock, 2010; Tijs et al., 2016) or tendon interactions (Tijs et al., 2014) can occur. In this study, the impact of these two factors is likely to be minimal because the PL and GAS muscles both have minimal shortening during the recoil (see Fig. 1D) and then shorten with similar relative displacements during the isotonic phase, and in kangaroo rats, the PL and GAS tendons are completely mechanically separate (Javidi et al., 2019b) and thus do not interact (see Introduction). To separate the contributions of the LG and the MG, we also had to assume that their tendons were effectively independent, and as a consequence, the muscle length changes (as measured by sonomicrometry) were influenced by the apparent stiffness of the tendon attached to each muscle.

Because the two models provided different predictions for how the percent contribution of each muscle varies with isotonic level, we could test the validity of each model if we had an independent estimate of individual muscle force. The sonomicrometry measurements provided that independent estimate, but this methodology also had several key assumptions that were simplifications of the physiology involved. The main assumption was that the tendon had a constant stiffness throughout the range of forces. The non-linearity of tendon stiffness, specifically in the toe region of the stress–strain curve of the tendon properties, could affect the method of estimation of individual muscle contribution to the group muscle force. Specifically, the average stiffness value of the isometric phase (from passive to maximal isometric force) is likely to be lower than the stiffness value during the isotonic recoil phase (from maximal isometric force to a lower isotonic force), leading to an underestimation of the normalized isotonic force (see Eqns A1–A3). This would potentially shift the *F–V* curves (e.g. as shown in Fig. 3) upwards slightly, causing a larger estimate of V_{max}.

The statistical analysis indicated that the estimations of the properties by Mdl1 and Mdl2 were significantly different, and there were no significant differences between Mdl2 estimations of individual muscle properties and the sonomicrometry-based estimations (Table 2). The fact that the Mdl2 predictions agreed with the independently derived estimates of individual muscle *F–V* properties does support the use of MT models with the appropriate

architecture parameters to estimate the individual muscle properties from measured group properties.

Contribution of individual plantarflexor muscles to the group properties

The second model (Mdl2), which was the more accurate predictor of the individual muscle properties, predicted that an individual muscle's contribution changes with loading condition (Fig. 5F). The change in contribution is consistent with the effect of differences in muscle architecture, namely fiber length and pennation angle, which determined fiber velocity for a given muscle group velocity (Bodine et al., 1982; Segal et al., 1986; Spector et al., 1980; Wakahara et al., 2013).

The results presented here clearly indicate that the assumption of a constant contribution of a muscle to the *F–V* or *P–V* relationship throughout the entire range of isotonic loads or shortening velocities is not correct. Consistent with our results, *in vivo* measurements combined with optimization methods to estimate the individual muscle properties of the human plantarflexor (Hasson and Caldwell, 2012) indicated changes in the contribution of GAS and SOL muscles with the level of muscle group isotonic load. However, that study could not validate the results by independently obtained data as we did in this study, with the caveat that the methodology used to estimate muscle forces from the sonomicrometry data had several simplifying assumptions.

More generally, our results indicated that the contribution of the individual muscles to the group muscle force is not distributed entirely based on the PCSA of the muscles. This is consistent with the findings in the human wrist extensors, the extensor carpi radialis brevis and longus (ECRB and ECRL, respectively). The ECRB produces more extensor moment than the ECRL under isometric conditions, but the reverse is true at velocities nearer to maximal shortening velocity of the combined muscle group (Lieber et al., 1997). In kangaroo rats, PCSA of the PL is higher than that of the LG and MG muscles (Rankin et al., 2018). Our previous study (Javidi et al., 2019a) and this study show that the percent contribution of the PL can be lower than that of the MG and LG muscles at certain muscle group lengths or isotonic levels, respectively.

APPENDIX

As described in the experimental protocols, the muscle group was stretched to the optimum length and stimulated to produce the maximum isometric force in the group and its individual muscles. Assuming a tendon with linear stiffness, the maximum isometric force of individual muscles can be estimated as:

$$F_{\mathrm{M,max}} = k_{\mathrm{T}}(L_{\mathrm{T,o}} - L_{\mathrm{T,s}}), \tag{A1}$$

where k_{T} is the stiffness of individual tendons, and $L_{\mathrm{T,o}}$ and $L_{\mathrm{T,s}}$ are the individual tendon length after isometric contraction (Fig. 1, green solid line) and at slack length of the group muscle (F_{GRP}=0), respectively. This equation also assumes that the slack lengths of all the muscles are identical. After the initial isometric contraction, the muscle group force was dropped quickly to the isotonic level of the force, mostly through recoil of the tendons (Fig. 1, red solid line). To estimate the isotonic force levels of individual muscles after tendon recoil ($F_{\mathrm{M,isot}}$), the amount of change in individual tendon lengths from the isometric contraction to the isotonic condition was used:

$$F_{\mathrm{M,isot}} = k_{\mathrm{T}}(L_{\mathrm{T,isot}} - L_{\mathrm{T,o}}) + F_{\mathrm{M,max}}, \tag{A2}$$

where $L_{\mathrm{T,isot}}$ is the individual tendon length after tendon recoil. By using Eqns A1 and A2, the normalized isotonic force of individual muscles can be calculated as:

$$\frac{F_{\mathrm{M,isot}}}{F_{\mathrm{M,max}}} = 1 + \frac{(L_{\mathrm{T,isot}} - L_{\mathrm{T,o}})}{(L_{\mathrm{T,o}} - L_{\mathrm{T,s}})}. \tag{A3}$$

Theoretically, the amount of change in tendon length is equal to the change in MT length minus the change in muscle length. Therefore, we used the MT length change and change in crystal distance (equivalent to muscle length change) to calculate the change in tendon length for each muscle:

$$\Delta L_{\mathrm{T}} = \Delta L_{\mathrm{MT}} - \Delta L_{\mathrm{c}}. \tag{A4}$$

Note that because we placed the crystals as close as possible to the MT junctions, we assumed that ΔL_{c} is equal to the change in muscle length. Thus, by using Eqns A3 and A4, $F_{\mathrm{M,n}}$ can be calculated as:

$$F_{\mathrm{M,n}} = 1 + \frac{(\Delta L_{\mathrm{MT,o\text{-}isot}} - \Delta L_{\mathrm{c,o\text{-}isot}})}{(\Delta L_{\mathrm{MT,s\text{-}o}} - \Delta L_{\mathrm{c,s\text{-}p}} - \Delta L_{\mathrm{c,p\text{-}o}})}, \tag{A5}$$

which is presented as Eqn 8 in Materials and Methods.

Competing interests

The authors declare no competing or financial interests.

Author contributions

Conceptualization: M.J., C.P.M., D.C.L.; Methodology: M.J., C.P.M., D.C.L.; Software: M.J.; Validation: M.J., C.P.M., D.C.L.; Formal analysis: M.J., C.P.M., D.C.L.; Investigation: M.J., C.P.M., D.C.L.; Resources: M.J., C.P.M., D.C.L.; Data curation: M.J., C.P.M., D.C.L.; Writing - original draft: M.J.; Writing - review & editing: M.J., C.P.M., D.C.L.; Visualization: M.J., C.P.M., D.C.L.; Supervision: C.P.M., D.C.L.; Project administration: C.P.M., D.C.L.; Funding acquisition: C.P.M., D.C.L.

Funding

This work was supported by Army Research Office grant 66554-EG (D.C.L. and C.P.M.) and National Science Foundation grant 1553550 (C.P.M.).

References

Anderson, D. E., Madigan, M. L. and Nussbaum, M. A. (2007). Maximum voluntary joint torque as a function of joint angle and angular velocity: Model development and application to the lower limb. *J. Biomech.* **40**, 3105-3113. doi:10.1016/j.jbiomech.2007.03.022

Arellano, C. J., Gidmark, N. J., Konow, N., Azizi, E. and Roberts, T. J. (2016). Determinants of aponeurosis shape change during muscle contraction. *J. Biomech.* **49**, 1812-1817. doi:10.1016/j.jbiomech.2016.04.022

Askew, G. N. and Marsh, R. L. (1998). Optimal shortening velocity (V/Vmax) of skeletal muscle during cyclical contractions: length-force effects and velocity-dependent activation and deactivation. *J. Exp. Biol.* **201**, 1527-1540.

Azizi, E., Brainerd, E. L. and Roberts, T. J. (2008). Variable gearing in pennate muscles. *Proc. Natl. Acad. Sci. USA* **105**, 1745-1750. doi:10.1073/pnas.0709212105

Biewener, A. and Blickhan, R. (1988). Kangaroo rat locomotion: design for elastic energy storage or acceleration? *J. Exp. Biol.* **140**, 243-255.

Biewener, A. A. and Roberts, T. J. (2000). Muscle and tendon contributions to force, work and elastic energy savings: a comparative perspective *Exerc. Sport Sci. Rev.* **28**, 99-107.

Biewener, A. A., Blickhan, R., Perry, A. K., Heglund, N. C. and Taylor, C. R. (1988). Muscle forces during locomotion in kangaroo rats: force platform and tendon buckle measurements compared. *J. Exp. Biol.* **137**, 191-205.

Bodine, S. C., Roy, R. R., Meadows, D. A., Zernicke, R. F., Sacks, R. D., Fournier, M. and Edgerton, V. R. (1982). Architectural, histochemical, and contractile characteristics of a unique biarticular muscle: the cat semitendinosus. *J. Neurophysiol.* **48**, 192-201. doi:10.1152/jn.1982.48.1.192

Brown, I. E., Liinamaa, T. L. and Loeb, G. E. (1996). Relationships between range of motion, l(o), and passive force in five strap-like muscles of the feline hind limb. *J. Morphol.* **230**, 69-77. doi:10.1002/(SICI)1097-4687(199610)230:1<69::AID-JMOR6>3.0.CO;2-I

Caldwell, G. E. and Chapman, A. E. (1991). The general distribution problem: a physiological solution which includes antagonism. *Hum. Mov. Sci.* **10**, 355-392. doi:10.1016/0167-9457(91)90012-M

Close, R. I. (1972). Dynamic mammalian properties of skeletal muscles. *Physiol. Rev.* **52**, 129-197. doi:10.1152/physrev.1972.52.1.129

Cui, L., Perreault, E. J., Maas, H. and Sandercock, T. G. (2008). Modeling short-range stiffness of feline lower hindlimb muscles. *J. Biomech.* **41**, 1945-1952. doi:10.1016/j.jbiomech.2008.03.024
Cui, L., Maas, H., Perreault, E. J. and Sandercock, T. G. (2009). In situ estimation of tendon material properties: Differences between muscles of the feline hindlimb. *J. Biomech.* **42**, 679-685. doi:10.1016/j.jbiomech.2009.01.022
de Brito Fontana, H., won Han, S., Sawatsky, A. and Herzog, W. (2018). The mechanics of agonistic muscles. *J. Biomech* **79**, 15-20. doi:10.1016/j.jbiomech.2018.07.007
Dick, T. J. M., Biewener, A. A. and Wakeling, J. M. (2017). Comparison of human gastrocnemius forces predicted by Hill-type muscle models and estimated from ultrasound images. *J. Exp. Biol.* **220**, 1643-1653. doi:10.1242/jeb.154807
Epstein, M. and Herzog, W. (1998). *Theoretical Models of Skeletal Muscles*. Wiley.
Fukashiro, S., Rob, M., Ichinose, Y., Kawakami, Y. and Fukunaga, T. (1995). Ultrasonography gives directly but noninvasively elastic characteristic of human tendon in vivo. *Eur. J. Appl. Physiol. Occup. Physiol.* **71**, 555-557. doi:10.1007/BF00238560
Garner, B. A. and Pandy, M. G. (2003). Estimation of musculotendon properties in the human upper limb. *Ann. Biomed. Eng.* **31**, 207-220. doi:10.1114/1.1540105
Graffe, M., McGowan, C. P., Lin, D. C. and Tanner, B. C. W. (2017). Measuring force production and myosin expression in hopping muscles of the kangaroo rat. In *National Veterinary Scholars Symposium*, p. 149. Bethesda, MD: National Cancer Institute with the Association of American Veterinary Medical Colleges.
Hasson, C. J. and Caldwell, G. E. (2012). Effects of age on mechanical properties of dorsiflexor and plantarflexor muscles. *Ann. Biomed. Eng.* **40**, 1088-1101. doi:10.1007/s10439-011-0481-4
Hasson, C. J., Miller, R. H. and Caldwell, G. E. (2011). Contractile and elastic ankle joint muscular properties in young and older adults. *PLoS ONE* **6**, e15953. doi:10.1371/journal.pone.0015953
Herzog, W. (2017). Skeletal muscle mechanics: questions, problems and possible solutions. *J. Neuroeng. Rehabil.* **14**, 1-17. doi:10.1186/s12984-017-0310-6
Hill, A. V. (1938). The heat of shortening and the dynamic constants of muscle. *Proc. R. Soc. B Biol. Sci.* **126**, 136-195. doi:10.1098/rspb.1938.0050
Huijing, P. A. (1996). Important experimental factors for skeletal muscle modelling: non-linear changes of muscle length force characteristics as a function of degree of activity. *Eur. J. Morphol.* **34**, 47-54. doi:10.1076/ejom.34.1.47.13157
Ichinose, Y., Kawakami, Y., Ito, M., Kanehisa, H. and Fukunaga, T. (2000). In vivo estimation of contraction velocity of human vastus lateralis muscle during "isokinetic" action. *J. Appl. Physiol.* **88**, 851-856. doi:10.1152/jappl.2000.88.3.851
Javidi, M., McGowan, C. P. and Lin, D. C. (2019a). The contributions of individual muscle–tendon units to the plantarflexor group force–length properties. *Ann. Biomed. Eng.* **47**, 2168-2177. doi:10.1007/s10439-019-02288-z
Javidi, M., Mcgowan, C. P., Schiele, N. R. and Lin, D. C. (2019b). Tendons from kangaroo rats are exceptionally strong and tough. *Sci. Rep.* **9**, 8196. doi:10.1038/s41598-019-44671-9
Lieber, R. L., Ljung, B. O. and Fridén, J. (1997). Intraoperative sarcomere length measurements reveal differential design of human wrist extensor muscles. *J. Exp. Biol.* **200**, 19-25.
Maas, H. and Sandercock, T. G. (2010). Force transmission between synergistic skeletal muscles through connective tissue linkages. *J. Biomed. Biotechnol.* **2010**, 1-9. doi:10.1155/2010/575672
Maas, H., Baan, G. C. and Huijing, P. A. (2004). Muscle force is determined also by muscle relative position: Isolated effects. *J. Biomech.* **37**, 99-110. doi:10.1016/S0021-9290(03)00235-5
Marsh, R. L. and Bennett, A. F. (1986). Thermal dependence of contractile properties of skeletal muscle from the lizard Sceloporus occidentalis with comments on methods for fitting and comparing force-velocity curves. *J. Exp. Biol.* **126**, 63-77.
Matson, A., Konow, N., Miller, S., Konow, P. P. and Roberts, T. J. (2012). Tendon material properties vary and are interdependent among turkey hindlimb muscles. *J. Exp. Biol.* **215**, 3552-3558. doi:10.1242/jeb.072728
Medler, S. (2002). Comparative trends in shortening velocity and force production in skeletal muscles. *Am. J. Physiol. Regul. Integr. Comp. Physiol.* **283**, R368-R378. doi:10.1152/ajpregu.00689.2001
Mendez, J. and Keys, A. (1960). Density and composition of mammalian muscle. *Metabolism* **9**, 184-188.
Moo, E. K., Peterson, D. R., Leonard, T. R., Kaya, M. and Herzog, W. (2017). In vivo muscle force and muscle power during near-maximal frog jumps. *PLoS ONE* **12**, 1-15. doi:10.1371/journal.pone.0173415
Nelson, F. E., Gabaldon, A. M. and Roberts, T. J. (2004). Force – velocity properties of two avian hindlimb muscles. *Comp. Biochem. Physiol. A Mol. Integr. Physiol.* **137**, 711-721. doi:10.1016/j.cbpb.2004.02.004
Rajagopal, A., Dembia, C. L., Demers, M. S., Delp, D. D., Hicks, J. L. and Delp, S. L. (2015). Full body musculoskeletal model for muscle driven simulation of human gait. *IEEE Trans. Biomed. Eng.* **63**, 2068-2079. doi:10.1109/TBME.2016.2586891
Rankin, J. W., Doney, K. M. and McGowan, C. P. (2018). Functional capacity of kangaroo rat hindlimbs: adaptations for locomotor performance. *J. R. Soc. Interface* **15**, 20180303. doi:10.1098/rsif.2018.0303
Rehwaldt, J. D., Rodgers, B. D. and Lin, D. C. (2017). Skeletal muscle contractile properties in a novel murine model for limb girdle muscular dystrophy 2i. *J. Appl. Physiol.* **123**, 1698-1707. doi:10.1152/japplphysiol.00744.2016
Rijkelijkhuizen, J. M., Baan, G. C., de Haan, A., de Ruiter, C. J. and Huijing, P. A. (2005). Extramuscular myofascial force transmission for in situ rat medial gastrocnemius and plantaris muscles in progressive stages of dissection. *J. Exp. Biol.* **208**, 129-140. doi:10.1242/jeb.01360
Rospars, J. P. and Meyer-Vernet, N. (2016). Force per cross-sectional area from molecules to muscles: a general property of biological motors. *R. Soc. Open Sci.* **3**. doi:10.1098/rsos.160313
Rugg, S. G., Gregor, R. J., Mandelbaum, B. R. and Chiu, L. (1990). In vivo moment arm calculations at the ankle using magnetic resonance imaging (MRI). *J. Biomech.* **23**, 495-501. doi:10.1016/0021-9290(90)90305-M
Sawicki, G. S., Sheppard, P. and Roberts, T. J. (2015). Power amplification in an isolated muscle-tendon unit is load dependent. *J. Exp. Biol.* **218**, 3700-3709. doi:10.1242/jeb.126235
Schiaffino, S. and Reggiani, C. (2011). Fiber types in Mammalian skeletal muscles. *Physiol. Rev.* **91**, 1447-1531. doi:10.1152/physrev.00031.2010
Schwaner, M. J., Lin, D. C. and McGowan, C. P. (2018). Jumping mechanics of desert kangaroo rats. *J. Exp. Biol.* **221**, jeb186700. doi:10.1242/jeb.186700
Segal, S. S., White, T. P. and Faulkner, J. A. (1986). Architecture, composition, and contractile properties of rat soleus muscle grafts. *Am. J. Physiol. Cell Physiol.* **250**, C474-C479. doi:10.1152/ajpcell.1986.250.3.C474
Spector, S. A., Gardiner, P. F., Zernicke, R. F., Roy, R. R. and Edgerton, V. R. (1980). Muscle architecture and force-velocity characteristics of cat soleus and medial gastrocnemius: implications for motor control. *J. Neurophysiol.* **44**, 951-960. doi:10.1152/jn.1980.44.5.951
Swoap, S. J., Caiozzo, V. J. and Baldwin, K. M. (1997). Optimal shortening velocities for in situ power production of rat soleus and plantaris muscles. *Am. J. Physiol.* **273**, C1057-C1063. doi:10.1152/ajpcell.1997.273.3.C1057
Tijs, C., Van Dieën, J. H., Baan, G. C. and Maas, H. (2014). Three-dimensional ankle moments and nonlinear summation of rat triceps surae muscles. *PLoS ONE* **9**, e111595. doi:10.1371/journal.pone.0111595
Tijs, C., van Dieen, J. H. and Maas, H. (2015). No functionally relevant mechanical effects of epimuscular myofascial connections between rat ankle plantar flexors. *J. Exp. Biol.* **218**, 2935-2941. doi:10.1242/jeb.122747
Tijs, C., van Dieën, J. H., Baan, G. C. and Maas, H. (2016). Synergistic co-activation increases the extent of mechanical interaction between rat ankle plantar-flexors. *Front. Physiol.* **7**, 1-8. doi:10.3389/fphys.2016.00414
Wakahara, T., Kanehisa, H., Kawakami, Y., Fukunaga, T. and Yanai, T. (2013). Relationship between muscle architecture and joint performance during concentric contractions in humans. *J. Appl. Biomech.* **29**, 405-412. doi:10.1123/jab.29.4.405
Weis-Fogh, T. and Alexander, R. M. (1977). The sustained power output from striated muscle. In *Scale Effects in Animal Locomotion* (ed. T. J. Pedley), pp. 511-525. London: Academic Press.

Summary: Incorporating appropriate fiber properties and muscle architecture is necessary to evaluate the contribution of individual muscles to combined plantarflexor force–velocity properties.

Funding details

S.No.	Funder name	Funder ID	Grant ID
1	Army Research Office	http://dx.doi.org/10.13039/100000183	66554-EG
2	National Science Foundation	http://dx.doi.org/10.13039/100000001	1553550